Optimal control design for the nonlinear manoeuvrability of a submarine

Javier García[*] Diana M. Ovalle[†] and Francisco Periago[‡]

March 2, 2009

Abstract

A six degree of freedom (6-DOF) nonlinear mathematical model for a submarine is proposed. Then, the problem of manoeuvrability control for this vehicle is formulated as an unconstrained optimal control problem which is solved by using a gradient descent method. Simulation results presented are rooted by three requirements which are of a major importance in naval industry, and they are compared to a classical linear model.

Index terms. Manoeuvrability control, submarine, optimal control, gradient descent method.

1 Introduction

In the development of a naval architecture tool for the guidance and autopilot of a submarine is important to choose both an accurate mathematical model for the equations of motion and a suitable control strategy. In spite of the practical importance of this matter, there are not so much works available in the literature, probably because of its applications in military technology. In fact, most of the results which are used by naval industry are based on simplified (meanly linear) versions of more accurate nonlinear models or on nonlinear models with lower degrees of freedom. Nowadays, the following three challenges deserve an special attention at the practical level:

(i) optimality of sizing rudders (decision to be taken during the design state),

[*]Dirección de Ingeniería, DICA, Navantia S. A., 30205 Cartagena (Spain) - jgpelaez@navantia.es

[†]Departamento de Matemática Aplicada y Estadística, ETSI Industriales, Universidad Politécnica de Cartagena, 30202 Cartagena, Spain - diana.ovalle@upct.es. Supported by project 2113/07MAE from Navantia S. A. and 08720/PI/08 from Fundación Séneca.

[‡]Departamento de Matemática Aplicada y Estadística, ETSI Industriales, Universidad Politécnica de Cartagena, 30202 Cartagena, Spain - f.periago@upct.es. Supported by projects MTM2007-62945 from Ministerio de Ciencia y Tecnología (Spain), 08720/PI/08 from Fundación Séneca (Gobierno Regional de Murcia, Spain) and 21131/07MAE from Navantia S.A.

(ii) design of an automatic submarine autopilot to be able to guarantee smooth manoeuvres as physically admissible in order to reduce hydraulic oil consumption and so reduce noise generation, and

(iii) reduction of vulnerability due to excessive movements in complex scenarios (e.g., littoral waters, missile launching or aggressive mining).

Having this in mind, firstly, a vehicle dynamics model based on a combination of theory and empirical data is proposed in this work. Indeed, taking as a starting point the standard DTNSRDC nonlinear equations of motion for an underwater vehicle [5, 7, 9] and adapting these general equations to the particular characteristics of a prototype developed by the company Navantia S.A. Cartagena Shipyard (Spain), we propose a mathematical model composed of a highly coupled and nonlinear system of ordinary differential equations (ODEs) with six degrees of freedom.

The second aim of this work is to design numerically an appropriate nonlinear control system which may be used for simulation of the usual depth and course keeping manoeuvres (among others) as well as to provide some useful information to deal with the above three points (i)-(iii). To this end, we describe the controller design as an unconstrained optimal control problem and implement a gradient descent method to solve it. This is an iterative algorithm which requires a good initialization to get a rapid convergence. To achieve a good initialization and also for comparison purposes, we derive from the original nonlinear model a simplified (4-DOF) linear mathematical model and solve it by using classical results on controllability theory [8].

Finally, numerical results are given to show the resulting nonlinear manoeuvres comparing to the linear ones and also the result for nonlinear manoeuvres which cannot be done with the linear model because of its restrictions on the variables values.

2 Vehicle modeling

The three-dimensional equations of motion for a marine vehicle are usually described by using two coordinate frames: the moving coordinate frame which is fixed to the vehicle and is called the *body-fixed* reference frame, and the earth-fixed reference frame which is called the *world* reference frame. The origin of body coordinates is at the half point along the symmetric longitudinal axis. Typically, this point is not so far from the center of buoyancy (CB) and from the center of gravity (CG). The body axes are longitudinal pointing in the nominal forward direction of the vehicle, lateral pointing through the right hand side of the level vehicle, and downward through the nominal bottom of the vehicle. The world coordinate system is defined by three orthogonal axes originating at an arbitrary local point at the ocean surface. North corresponds to $x-$axis, East corresponds to $y-$axis and increasing depth

corresponds to $z-$axis. The position and orientation of the vehicle are described in the world system while the linear and angular velocities are expressed in the body-fixed coordinate system. These quantities are defined according to SNAME notation [7] as:

$$\eta(t) = [\eta_1^*(t), \eta_2^*(t)], \quad \eta_1(t) = [x(t), y(t), z(t)]^*, \quad \eta_2(t) = [\phi(t), \theta(t), \psi(t)]^*$$

$$\nu(t) = [\nu_1^*(t), \nu_2^*(t)], \quad \nu_1 = [u(t), v(t), w(t)]^*, \qquad \nu_2(t) = [p(t), q(t), r(t)]^*. \tag{1}$$

Here a^* stands for the transpose of vector a, η_1 denotes the position of the vehicle in the world system, η_2 is the orientation in the same reference system, ν_1 is the vector of linear velocities in the body-fixed frame (where as usual u is surge velocity, v is sway velocity, and w is heave velocity), and finally ν_2 is the vector of angular velocities in the body-fixed reference system (p is roll rate, q is pitch rate, and r is yaw rate). We refer to [7] for a detailed description of these two reference frames as well as the variables $\eta(t)$ and $\nu(t)$.

The kinematic equations which relate the body-fixed reference frame to the world reference system can be expressed in vector form as:

$$\begin{bmatrix} \dot{\eta}_1 \\ \\ \dot{\eta}_2 \end{bmatrix} = \begin{bmatrix} J_1(\eta_2) & 0_{3\times3} \\ \\ 0_{3\times3} & J_2(\eta_2) \end{bmatrix} \begin{bmatrix} \nu_1 \\ \\ \nu_2 \end{bmatrix} \tag{2}$$

where dot means derivative with respect to time, and the matrices $J_1(\eta_2)$ and $J_2(\eta_2)$ are given respectively by

$$J_1(\eta_2) = \begin{bmatrix} \cos\psi\cos\theta & -\sin\psi\cos\theta + \cos\psi\sin\theta\sin\phi & \sin\psi\sin\phi + \cos\psi\cos\phi\sin\theta \\ \sin\psi\cos\theta & \cos\psi\cos\phi + \sin\phi\sin\theta\sin\psi & -\cos\psi\sin\phi + \sin\theta\sin\psi\cos\phi \\ -\sin\theta & \cos\theta\sin\phi & \cos\theta\cos\phi \end{bmatrix} \tag{3}$$

and

$$J_2(\eta_2) = \begin{bmatrix} 1 & \sin\phi\tan\theta & \cos\phi\tan\theta \\ 0 & \cos\phi & -\sin\phi \\ & \sin\phi/\cos\theta & \cos\phi/\cos\theta \end{bmatrix}. \tag{4}$$

The dynamic equations of motion can be derived from a Newton-Euler formulation which is based on Newton's second law. The development of the functional form of the hydrodynamic forces and moments is by now well-known [5, 7, 9]. Specific values of the particular hydrodynamic coefficients which appear in the equations depend on the specific vehicle and, therefore, would require modification if applied to other vehicles. The values of the coefficients used in this work have been experimentally obtained in deeply submerged conditions by using the scaling model showed in Figure 1 and are listed in Appendix. A detailed study of the mentioned model as well as several captive manoeuvring tests appear in the internal report [2].

Figure 1: Appearance of the model studied in this work (picture taken from [2]).

According to these considerations, the dynamics equations of motion for the specific submarine considered in this work read as follows:

AXIAL FORCE EQUATION:

$$\begin{aligned} & m[\dot{u} - vr + wq - x_G(q^2 + r^2) + y_G(pq - \dot{r}) + z_G(pr + \dot{q})] \\ = \; & \frac{\rho}{2} l^4 [X'_{qq} q^2 + X'_{rr} r^2 + X'_{rp} rp + X'_{q|q|} q|q|] + \frac{\rho}{2} l^3 [X'_{\dot{u}} \dot{u} + X'_{vr} vr + X'_{wq} wq] \\ & + \frac{\rho}{2} l^2 [X'_{uu} u^2 + X'_{vv} v^2 + X'_{ww} w^2 + X'_{w|w|} w|w|] \\ & + \frac{\rho}{2} l^2 [X'_{\delta_r \delta_r} u^2 \delta_r^2 + X'_{\delta_s \delta_s} u^2 \delta_s^2 + X'_{\delta_b \delta_b} u^2 \delta_b^2] - (W - B)\sin(\theta) \\ & + \rho T (1 - t) \end{aligned} \tag{5}$$

where

$$\begin{aligned} T \; = \; & \left(K_{T0} + K_{TJ} \frac{(1 - w_f)}{nD} u + K_{TJ^2} \frac{(1 - w_f)^2}{(nD)^2} u^2 \right. \\ & \left. + K_{TJ^3} \frac{(1 - w_f)^3}{(nD)^3} u^3 + K_{TJ^4} \frac{(1 - w_f)^4}{(nD)^4} u^4 \right) n^2 D^4 \end{aligned}$$

LATERAL FORCE EQUATION:

$$\begin{aligned} & m[\dot{v} - wp + ur - y_G(r^2 + p^2) + z_G(qr - \dot{p}) + x_G(qp + \dot{r})] \\ = \; & \frac{\rho}{2} l^4 [Y_{\dot{r}}^{'} \dot{r} + Y_{\dot{p}}^{'} \dot{p} + Y_{r|r|}^{'} r|r| + Y_{pq}^{'} pq] \\ & + \frac{\rho}{2} l^3 [Y_r^{'} ur + Y_p^{'} up + Y_{\dot{v}}^{'} \dot{v} + Y_{wp}^{'} wp] \\ & + \frac{\rho}{2} l^2 [Y_*^{'} u^2 + Y_v^{'} uv + Y_{v|v|N}^{'} v|(v^2 + w^2)^{\frac{1}{2}}|] \\ & + \frac{\rho}{2} l^2 [Y_{\delta_r}^{'} u^2 \delta_r + Y_{\delta_r \eta}^{'} u^2 \delta_r (\eta - \frac{1}{C}) C] \\ & + \frac{\rho}{2} l^2 Y_{vwN}^{'} vw + (W - B)\cos(\theta)\sin(\phi) \end{aligned} \tag{6}$$

NORMAL FORCE EQUATION:

$$\begin{aligned} & m[\dot{w} - uq + vp - z_G(p^2 + q^2) + x_G(rp - \dot{q}) + y_G(rq + \dot{p})] \\ = \; & \frac{\rho}{2} l^4 [Z_{\dot{q}}^{'} \dot{q} + Z_{q|q|}^{'} q|q| + Z_{rr}^{'} r^2] + \frac{\rho}{2} l^3 [Z_{\dot{w}}^{'} \dot{w} + Z_q^{'} uq + Z_{vp}^{'} vp + Z_{vr}^{'} vr] \\ & + \frac{\rho}{2} l^2 [Z_*^{'} u^2 + Z_w^{'} uw + Z_{vv}^{'} v^2] \\ & + \frac{\rho}{2} l^2 [Z_{|w|}^{'} u|w| + Z_{wwN}^{'} \left| w(v^2 + w^2)^{\frac{1}{2}} \right|] \\ & + \frac{\rho}{2} l^2 \left[Z_{\delta_s}^{'} u^2 \delta_s + Z_{\delta_b}^{'} u^2 \delta_b + Z_{\delta_s \eta}^{'} u^2 \delta_s \left(\eta - \frac{1}{C} \right) C \right] \\ & + (W - B)\cos(\theta)\cos(\phi) \end{aligned} \tag{7}$$

ROLLING MOMENT EQUATION:

$$\begin{aligned} & I_x \dot{p} + (I_z - I_y) qr - I_{zx} \dot{r} - I_{zx} pq + I_{yz} r^2 - I_{yz} q^2 + I_{xy} pr - I_{xy} \dot{q} \\ & m y_G \dot{w} - m y_G uq + m y_G vp - m z_G \dot{v} + m z_G wp - m z_G ur \\ = \; & \frac{\rho}{2} l^5 K_{\dot{p}}^{'} \dot{p} + \frac{\rho}{2} l^5 K_{\dot{r}}^{'} \dot{r} + \frac{\rho}{2} l^5 K_{qr}^{'} qr + \frac{\rho}{2} l^5 K_{p|p|}^{'} p|p| + \frac{\rho}{2} l^5 K_{r|r|}^{'} r|r| \\ & + \frac{\rho}{2} l^4 K_p^{'} up + \frac{\rho}{2} l^4 K_r^{'} ur + \frac{\rho}{2} l^4 K_{\dot{v}}^{'} \dot{v} + \frac{\rho}{2} l^4 K_{wp}^{'} wp \\ & + \frac{\rho}{2} l^3 K_*^{'} u^2 + \frac{\rho}{2} l^3 K_v^{'} uv + \frac{\rho}{2} l^3 K_{v|v|}^{'} v|v| + \frac{\rho}{2} l^3 K_{\delta_r}^{'} u^2 \delta_r \\ & + (Y_G W - Y_B B)\cos(\theta)\cos(\phi) - (Z_G W - Z_B B)\cos(\theta)\sin(\phi) \\ & - \rho Q \end{aligned} \tag{8}$$

$$\tag{9}$$

where

$$\begin{aligned} Q \; = \; & \left(K_{Q0} + K_{QJ} \frac{(1 - w_f)}{nD} u + K_{QJ^2} \frac{(1 - w_f)^2}{(nD)^2} u^2 \right. \\ & \left. + K_{QJ^3} \frac{(1 - w_f)^3}{(nD)^3} u^3 + K_{QJ^4} \frac{(1 - w_f)^4}{(nD)^4} u^4 \right) n^2 D^5 \end{aligned}$$

PITCHING MOMENT EQUATION:

$$\begin{aligned} & I_y\dot{q} + (I_x - I_z)rp - (\dot{p} + qr)I_{xy} + (p^2 - r^2)I_{zx} + (qp - \dot{r})I_{yz} \\ & +m[z_G(\dot{u} - vr + wq) - x_G(\dot{w} - uq + vp)] \\ = \; & \frac{\rho}{2}l^5[M_{\dot{q}}^{'}\dot{q} + M_{rp}^{'}rp + M_{q|q|}^{'}q|q| + M_{rr}^{'}r^2] + \frac{\rho}{2}l^4[M_{\dot{w}}^{'}\dot{w} + M_{q}^{'}uq + M_{vr}^{'}vr] \\ & +\frac{\rho}{2}l^3\left[M_{*}^{'}u^2 + M_{w}^{'}uw + M_{vv}^{'}v^2 + M_{w|w|N}^{'}w\left|(v^2+w^2)^{\frac{1}{2}}\right|\right] \\ & +\frac{\rho}{2}l^3[M_{vw}^{'}vw + M_{|w|}^{'}u|w| + M_{ww}^{'}|w(v^2+w^2)^{\frac{1}{2}}|] \\ & +\frac{\rho}{2}l^3\left[M_{\delta_s}^{'}u^2\delta_s + M_{\delta_b}^{'}u^2\delta_b + M_{\delta_s\eta}^{'}u^2\delta_s\left(\eta - \frac{1}{C}\right)C\right] \\ & -(x_GW - x_BB)\cos(\theta)\cos(\phi) - (z_GW - z_BB)\sin(\theta) \end{aligned} \tag{10}$$

YAWING MOMENT EQUATION:

$$\begin{aligned} & I_z\dot{r} + (I_y - I_x)pq - (\dot{q} + rp)I_{yz} + (q^2 - p^2)I_{xy} + (rq - \dot{p})I_{zx} \\ & +m[x_G(\dot{v} - wp + ur) - y_G(\dot{u} - vr + wq)] \\ = \; & \frac{\rho}{2}l^5[N_{\dot{r}}^{'}\dot{r} + N_{r|r|}^{'}r|r| + N_{\dot{p}}^{'}\dot{p} + N_{pq}^{'}pq] + \frac{\rho}{2}l^4[N_{p}^{'}up + N_{r}^{'}ur + N_{\dot{v}}^{'}\dot{v}] \\ & +\frac{\rho}{2}l^3[N_{*}^{'}u^2 + N_{v}^{'}uv + N_{v|v|N}^{'}v\left|(v^2+w^2)^{\frac{1}{2}}\right|] \\ & +\frac{\rho}{2}l^3\left[N_{\delta_r}^{'}u^2\delta_r + N_{\delta_r\eta}^{'}u^2\delta_r\left(\eta - \frac{1}{C}\right)C\right] \\ & +\frac{\rho}{2}l^3N_{vwN}^{'}vw \\ & +(x_GW - x_BB)\cos(\theta)\sin(\phi) + (y_GW - y_BB)\sin(\theta) \end{aligned} \tag{11}$$

These equations include the functional form of both mechanical and hydrodynamic added mass, coriolis and centripetal forces, damping forces and moments due to skin friction and vortex shedding, restoring (i.e., gravitation and buoyant) forces and moments, propeller forces and moments, and rudders control forces. We refer to [7, 10] for a detailed description and analysis of these forces and moments.

For the specific vehicle considered in this work, control inputs come in the form of thruster forces and moments and may be expressed as a vector

$$\mathbf{u}(t) = [\delta_b(t), \delta_s(t), \delta_r(t)], \tag{12}$$

where δ_b is deflection of bow plane, δ_s is deflection of stern plane, and δ_r is deflection of rudder.

From a pure mathematical point of view, it is important to point out the following facts in the proposed model:

- The high nonlinear character of the equations and the high order of the system (12 equations).

- The lack of differentiability of the system which is caused for several terms involving non-differentiable functions such as the absolute value and squared roots.
- The controls appear in nonlinear (quadratic) form.

Because of these three difficulties, it is certainly hard to study the model at the pure mathematical level (existence, uniqueness of solutions, etc.). Indeed, very few is known in the mathematical literature concerning to the control of non-differentiable systems with controls appearing in nonlinear form. We refer to [3] for a recent related paper. Since this work is mainly addressed to numerical simulations and application to a real-life engineering problem, we do not enter here in the above theoretical question which, however, will be analyzed in a future work.

Both kinematic equations (2) and dynamic equations (5)-(11) are the equations of motion for the submarine. It is convenient to write down these equations in a more compact form. To this end, we introduce the state vector

$$\mathbf{x}(t) = [x(t), y(t), z(t), \phi(t), \theta(t), \psi(t), u(t), v(t), w(t), p(t), q(t), r(t)].$$

After some simple algebra, the set of equations (2) and (5)-(11) can be rewritten in the form

$$\mathbf{M}\,\dot{\mathbf{x}}(t) = \widetilde{\mathbf{f}}(\mathbf{x}(t), \mathbf{u}(t)) \tag{13}$$

where the matrix $\mathbf{M}$ is given by

$$\mathbf{M} = \begin{bmatrix} \mathbf{1}_{6\times 6} & \mathbf{0}_{6\times 6} \\ \mathbf{0}_{6\times 6} & \mathbf{M}' \end{bmatrix} \tag{14}$$

and

$$\mathbf{M}' = \begin{bmatrix} \mathbf{M}'_{\mathbf{1}} & \mathbf{M}'_{\mathbf{2}} \end{bmatrix}$$

where

$$\mathbf{M}'_{\mathbf{1}} = \begin{bmatrix} m - \frac{\rho l^3}{2} X'_{\dot{u}} & 0 & 0 \\ 0 & m - \frac{\rho l^3}{2} Y'_{\dot{v}} & 0 \\ 0 & 0 & 0 \\ 0 & -\left(\frac{\rho}{2} l^4 K'_{\dot{v}} + m z_G\right) & m y_G \\ m z_G & 0 & -\left(\frac{\rho l^4}{2} M'_{\dot{w}} + m x_G\right) \\ -m y_G & m x_G - \frac{\rho l^4}{2} N'_{\dot{v}} & 0 \end{bmatrix}$$

and

$$\mathbf{M_2'} = \begin{bmatrix} 0 & mz_G & -my_G \\ -\left(\frac{\rho l^4}{2} Y'_{\dot{p}} + mz_G\right) & 0 & mx_G - \frac{\rho l^4}{2} Y'_{\dot{r}} \\ m - \frac{\rho l^3}{2} Z'_{\dot{w}} & -\left(\frac{\rho l^4}{2} Z'_{\dot{q}} + mx_G\right) & my_G \\ I_x - \frac{\rho l^5}{2} K'_{\dot{p}} & -I_{xy} & -\left(\frac{\rho l^5}{2} K'_{\dot{r}} + I_{zx}\right) \\ -I_{xy} & I_y - \frac{\rho l^5}{2} M'_{\dot{q}} & -I_{yz} \\ -\left(\frac{\rho l^5}{2} N'_{\dot{p}} + I_{zx}\right) & -I_{yz} & I_z - \frac{\rho l^5}{2} N'_{\dot{r}} \end{bmatrix}$$

Since $\mathbf{M}$ is invertible, (13) transforms into

$$\dot{\mathbf{x}}(t) = \mathbf{f}(\mathbf{x}(t), \mathbf{u}(t)) \tag{15}$$

where $\mathbf{f} = \mathbf{M}^{-1}\widetilde{\mathbf{f}}$.

Once we have at our disposal the equations of motion for the underwater vehicle, we are in a position to design a controller to simulate arbitrary manoeuvres.

3 Nonlinear controller design

The control problem can be formulated as follows: given an initial state $\mathbf{x}(0) = \mathbf{x}^0 \in \mathbb{R}^{12}$ and a desired final target $\mathbf{x}^T$, the goal is to calculate the vector of control $\mathbf{u}(t)$ which is able to draw our system from the initial state $\mathbf{x}^0$ to (or near to) the final one $\mathbf{x}^T$ in a given time T. In mathematical terms, this problem may be formulated as the unconstrained optimal control problem

$$\begin{cases} \text{Minimize in } \mathbf{u}: & J(\mathbf{u}) = \Phi\left(\mathbf{x}(T), \mathbf{x}^T\right) + \int_0^T F(\mathbf{x}(t), \mathbf{u}(t))\, dt \\ \text{subject to} & \\ & \dot{\mathbf{x}}(t) = \mathbf{f}(\mathbf{x}(t), \mathbf{u}(t)) \\ & \mathbf{x}(0) = \mathbf{x}^0 \end{cases} \tag{16}$$

Here $\Phi\left(\mathbf{x}(T), \mathbf{x}^T\right)$ and $F(\mathbf{x}(t), \mathbf{u}(t))$ are two generic functions which can be chosen as desired. At this point, a pair of remarks is in order:

- It is evident that the original problem includes some constraints on both the control inputs and the state variables. This is very important in order to choose an appropriate numerical control method but, at the practical point of view, all of these restrictions can be easily satisfied by taking the final time T large enough. For this reason, in this preliminary work we will not consider the above mentioned constraints.
- As for the cost function $J(\mathbf{u})$, we have written it in a general format because the method we plan to develop in the remaining can be applied in this general

setting. Concerning to the particular problem of control of the manoeuvrability for an underwater vehicle, which is the main goal of this work, it is quite natural to take

$$\Phi\left(\mathbf{x}\left(T\right),\mathbf{x}^{T}\right)=\sum_{j=1}^{12}\alpha_{j}\left(\mathbf{x}_{j}\left(T\right)-\mathbf{x}_{j}^{T}\right)^{2} \tag{17}$$

with $\alpha_j > 0$ penalty parameters, and

$$F\left(\mathbf{x}\left(t\right),\mathbf{u}\left(t\right)\right)=\sum_{j=1}^{3}\beta_{j}\left(\mathbf{u}_{j}\left(t\right)\right)^{2} \tag{18}$$

with $\beta_j > 0$ another weight parameters. Therefore, the cost function $J(\mathbf{u})$ is a commitment between reaching the final target and a minimal expense of control on having done the corresponding manoeuvre.

There are several optimization methods which can be applied to solve (16). Due to the complexity of the state law and the large number of variables involved in the problem, it is quite reasonable to use a gradient descent method. Briefly, the scheme of this method consists of the following main steps:

- Initialization of the control input $\mathbf{u}^0$.
- For $k \geq 0$, iteration until convergence (e.g. $\left|J\left(\mathbf{u}^{k+1}\right)-J\left(\mathbf{u}^{k}\right)\right| \leq \varepsilon\left|J\left(\mathbf{u}^{0}\right)\right|$, with $\varepsilon > 0$ a suitable tolerance) as follows:

$$\mathbf{u}^{k+1}=\mathbf{u}^{k}-\lambda\nabla J\left(\mathbf{u}^{k}\right)$$

where $\lambda > 0$ is a fixed step parameter, and $\nabla J\left(\mathbf{u}^{k}\right)$ is the gradient of the cost function.

The crucial step is the computation of the gradient $\nabla J\left(\mathbf{u}^{k}\right)$. This can be obtained by using the adjoint method which is described next:

1. Given the control $\mathbf{u}^k$, $k \geq 0$, solve the state equation

$$\begin{cases}\dot{\mathbf{x}}\left(t\right)=\mathbf{f}\left(\mathbf{x}\left(t\right),\mathbf{u}^{k}\left(t\right)\right)\\ \mathbf{x}\left(0\right)=\mathbf{x}^{k}\left(0\right)\end{cases}$$

to obtain the state $\mathbf{x}^{k+1}(t)$.

2. With the pair $\left(\mathbf{u}^{k}\left(t\right),\mathbf{x}^{k+1}\left(t\right)\right)$, solve the linear backward equation for the adjoint state $\mathbf{p}(t)$

$$\begin{cases}\dot{\mathbf{p}}\left(t\right)=-\nabla_{\mathbf{x}}\mathbf{F}\left(\mathbf{x}^{k+1}\left(t\right),\mathbf{u}^{k}\left(t\right)\right)-\left[\nabla_{\mathbf{x}}\mathbf{f}\left(\mathbf{x}^{k+1}\left(t\right),\mathbf{u}^{k}\left(t\right)\right)\right]^{*}\mathbf{p}\left(t\right)\\ \mathbf{p}\left(T\right)=\dot{\Phi}\left(\mathbf{x}^{k+1}\left(T\right),\mathbf{x}^{T}\right)\end{cases}$$

where $\nabla_{\mathbf{x}}$ is the gradient with respect to the state variable $\mathbf{x}$. Thus, we obtain $\mathbf{p}^{k+1}(t)$.

3. Finally,

$$\nabla J\left(\mathbf{u}^k\right) = \nabla_{\mathbf{u}}\mathbf{F}\left(\mathbf{x}^{k+1}(t), \mathbf{u}^k(t)\right) + \left[\nabla_{\mathbf{u}}\mathbf{f}\left(\mathbf{x}^{k+1}(t), \mathbf{u}^k(t)\right)\right]^* \mathbf{p}^{k+1}(t)$$

where now $\nabla_{\mathbf{u}}$ is the gradient with respect to $\mathbf{u}$.

Here $\mathbf{A}^*$ stands for the transpose of $\mathbf{A}$. We refer to [1, 4] for more details on this method. A main drawback of a gradient algorith is the low speed of convergence. This difficulty can be overcome by choosing a good initialization for the algorithm. For this reason and also to be able to compare results obtained from the above nonlinear model with more common linear models, we present and study a linear model in the next section.

4 Initialization of the nonlinear controller: A linear model

The material of this section has been essentially taken from [8], but for the sake of completeness we include it here. Taking as a starting point the set of equations (2) and (5)-(11), and making the additional assumptions:

- constant surge velocity u_0,
- deeply submerged conditions,
- small variations in pitch and yaw Euler angles, and
- some particular geometrical hypotheses on the submarine,

we obtain a mathematical linear model in the form

$$\begin{cases} \dot{\overline{\mathbf{x}}}(t) = \mathbf{A}\overline{\mathbf{x}}(t) + \mathbf{B}\overline{\mathbf{u}}(t) \\ \overline{\mathbf{x}}(0) = \overline{\mathbf{x}}^0 \end{cases} \tag{19}$$

where t is the time variable,

$$\overline{\mathbf{x}}(t) = \left[\overline{v}(t), \overline{r}(t), \overline{\psi}(t), \overline{y}(t), \overline{w}(t), \overline{q}(t), \overline{\theta}(t), \overline{z}(t)\right]$$

is the state variables vector (as before, here $\overline{v}$ is sway velocity, $\overline{r}$ yaw rate, $\overline{\psi}$ yaw Euler angle, $\overline{y}$ position along y-axis, $\overline{w}$ heave velocity, $\overline{q}$ pitch rate, $\overline{\theta}$ pitch Euler angle, and $\overline{z}$ is depth),

$$\overline{\mathbf{u}}(t) = \left[\overline{\delta}_b(t), \overline{\delta}_s(t), \overline{\delta}_r(t)\right],$$

is the control variables vector (with $\overline{\delta}_b$ deflection of bow plane, $\overline{\delta}_s$ deflection of stern plane, and $\overline{\delta}_r$ deflection of rudder), $\mathbf{A}$ is a 8×8 matrix and $\mathbf{B}$ is a 8×3 matrix. Precisely,

$$\mathbf{A} = \overline{\mathbf{M}}^{-1}\overline{\mathbf{B}}, \qquad \mathbf{B} = \overline{\mathbf{M}}^{-1}\overline{\mathbf{C}}$$

where

$$\overline{\mathbf{M}} = \begin{bmatrix} m' - Y'_{\dot{v}} & -Y'_{\dot{r}}\frac{l\pi}{180} & 0 & 0 & 0 & 0 & 0 & 0 \\ -N'_{\dot{v}} & m'\left(k_{zz}^2 - N'_{\dot{r}}\right)\frac{l\pi}{180} & 0 & 0 & 0 & 0 & 0 & 0 \\ 0 & 0 & 1 & 0 & 0 & 0 & 0 & 0 \\ 0 & 0 & 0 & 1 & 0 & 0 & 0 & 0 \\ 0 & 0 & 0 & 0 & m' - Z'_{\dot{w}} & -Z'_{\dot{q}}l & 0 & 0 \\ 0 & 0 & 0 & 0 & -M'_{\dot{w}} & m'(k_{yy}^2 - M'_{\dot{q}})\frac{l\pi}{180} & 0 & 0 \\ 0 & 0 & 0 & 0 & 0 & 0 & 1 & 0 \\ 0 & 0 & 0 & 0 & 0 & 0 & 0 & 1 \end{bmatrix},$$

$$\overline{\mathbf{B}} = \begin{bmatrix} Y'_v\frac{u_0}{l} & (Y'_r - m')\frac{u_0\pi}{180} & 0 & 0 & 0 & 0 & 0 & 0 \\ N'_v\frac{u_0}{l} & N'_r\frac{u_0\pi}{180} & 0 & 0 & 0 & 0 & 0 & 0 \\ 0 & 1 & 0 & 0 & 0 & 0 & 0 & 0 \\ 1 & 0 & \frac{u_0\pi}{180} & 0 & 0 & 0 & 0 & 0 \\ 0 & 0 & 0 & 0 & Z'_w\frac{u_0}{l} & \left(Z'_q + m'\right)\frac{u_0\pi}{180} & 0 & 0 \\ 0 & 0 & 0 & 0 & M'_w\frac{u_0}{l} & M'_q\frac{u_0\pi}{180} & -\frac{2}{\rho l^4}\left(Z_G W - Z_B B\right)\frac{\pi}{180} & 0 \\ 0 & 0 & 0 & 0 & 0 & 1 & 0 & 0 \\ 0 & 0 & 0 & 0 & 1 & 0 & -\frac{u_0\pi}{180} & 0 \end{bmatrix},$$

and

$$\overline{\mathbf{C}} = \begin{bmatrix} Y'_{\delta_r}\frac{u_0^2\pi}{l180} & 0 & 0 \\ N'_{\delta_r}\frac{u_0^2\pi}{l180} & 0 & 0 \\ 0 & 0 & 0 \\ 0 & 0 & 0 \\ 0 & Z'_{\delta_s}\frac{u_0^2\pi}{l180} & Z'_{\delta_b}\frac{u_0^2\pi}{l180} \\ 0 & M'_{\delta_s}\frac{u_0^2\pi}{l180} & M'_{\delta_b}\frac{u_0^2\pi}{l180} \\ 0 & 0 & 0 \\ 0 & 0 & 0 \end{bmatrix}.$$

The dimensionless linear hydrodynamic coefficients which appear in these matrices where obtained in [2] and are listed in the following table.

$m' = 1.71e-02$	$Y'_{\dot{v}} = -1.80e-02$	$Y'_{\dot{r}} = -8.30e-04$
$L = 60$	$N'_{\dot{v}} = 6.80e-04$	$k_{zz} = 0.849$
$N'_{\dot{r}} = -8.14e-04$	$Z'_{\dot{w}} = -1.46e-02$	$Z'_{\dot{q}} = -7.00e-05$
$M'_{\dot{w}} = -1.40e-03$	$k_{yy} = 1.047$	$M'_{\dot{q}} = -6.37e-04$
$Y'_v = 0$	$u_0 = 8$	$Y'_r = 0$
$N'_v = -2.30e-02$	$N'_r = 0$	$Z'_w = 0$
$Z'_q = 0$	$M'_w = 6.26e-03$	$M'_q = 0$
$\rho = 1000$	$Z_g = 0.089$	$W = 435$
$Z_b = 0$		$B = 435$
$Y'_{\delta_r} = 9.03e-03$	$N'_{\delta_r} = -4.06e-03$	$Z'_{\delta_s} = -6.25e-03$
$M'_{\delta_s} = -2.45e-03$	$Z'_{\delta_b} = -3.19e-03$	$M'_{\delta_b} = 6.38e-04$

Next, we recall the linear controllability problem (**LCP**) we are interested in:

(LCP) For a fixed final time T and given an initial state $\overline{\mathbf{x}}^0 \in \mathbb{R}^8$ and a final state $\overline{\mathbf{x}}^T \in \mathbb{R}^8$, we wonder if there exists a control variable $\overline{\mathbf{u}}(t)$, $0 \leq t \leq T$, such that the solution of (19) is driven from $\overline{\mathbf{x}}^0$ to $\overline{\mathbf{x}}^T$ at time T, i.e.,

$$\overline{\mathbf{x}}(0) = \overline{\mathbf{x}}^0 \quad \text{and} \quad \overline{\mathbf{x}}(T) = \overline{\mathbf{x}}^T.$$

By using linear finite-dimensional controllability theory it is not so hard to show that this problem has a positive answer**.** Indeed, as is well-known (see for instance [11]), the linear system (19) is exactly controllable at time T if and only if the controllability matrix

$$\mathbf{Q}_C = \left[\mathbf{B}\ \mathbf{AB}\ \mathbf{A}^2\mathbf{B}\ \cdots\cdots\ \mathbf{A}^7\mathbf{B}\right]$$

has maximal range. In our situation, it is very easy to see that this is so, i.e., the range of $\mathbf{Q}_C$ is equal to 8. Moreover, when controllability holds, the control $\overline{\mathbf{u}}(t)$ is explicitly given by

$$\overline{\mathbf{u}}(t) = \mathbf{B}^* e^{\mathbf{A}^*(T-t)} \left[\mathbf{P}(T)\right]^{-1} \left(\overline{\mathbf{x}}^T - e^{\mathbf{A}T}\overline{\mathbf{x}}^0\right), \quad 0 \leq t \leq T, \tag{20}$$

where $\mathbf{A}^*$, $\mathbf{B}^*$ are the transposes of $\mathbf{A}$ and $\mathbf{B}$, respectively, $e^{\mathbf{A}T}$ is the exponential matrix of $\mathbf{A}T$, and $\left[\mathbf{P}(T)\right]^{-1}$ is the inverse of the controllability Gramiam matrix

$$\mathbf{P}(T) = \int_0^T e^{\mathbf{A}T}\mathbf{B}\mathbf{B}^* e^{\mathbf{A}^* t} dt. \tag{21}$$

Once the control $\overline{\mathbf{u}}(t)$ is determined, the solution $\overline{\mathbf{x}}(t)$ of (19) is obtained in the closed form

$$\overline{\mathbf{x}}(t) = e^{\mathbf{A}t}\overline{\mathbf{x}}^0 + \int_0^t e^{\mathbf{A}(t-s)} B\overline{\mathbf{u}}(s)\, ds. \tag{22}$$

It is also important to notice that the control (20) is optimal in the sense that it is the one of minimal $L^2\left(0, T; \mathbb{R}^3\right)$-norm (see [6]).

5 Numerical simulations

In this section, we show some numerical results obtained by implementing the approach described in the preceding sections in Matlab® for realistic manoeuvres like depth change and turning. At each iteration the state and adjoint state equations have been solved by using the ODE45 Matlab function, which is a one-step solver based on an explicit Runge-Kutta (4,5) formula (see [12]). Our goal is to provide some useful numerical information to address challenges (i)-(iii) described in the introduction. For a depth change manoeuvre, we consider two different cases:

Case 1. In order to study *optimality of sizing rudders* (which is a typical example of a pre-contract navy requirement) we take:

$$\begin{cases} \lambda = 0.001 \qquad \varepsilon = 10^{-6} \\ \alpha_2 = \alpha_3 = \alpha_5 = 1, \quad \alpha_j = 0, \ j \neq 2,3,5 \\ \beta_j = 0, \ j = 1,2,3 \\ \mathbf{x}(0) = (0,0,400,0,0,0,2.5,0,0,0,0,0) \\ \mathbf{x}^T = (0,0,50,0,0,0,0,0,0,0,0,0), \quad T = 200. \end{cases} \tag{23}$$

That is, we penalize only the final value for the state variables $y(t), z(t)$ and $\theta(t)$. We want the submarine goes from a depth of $400m$ to $50m$ and, in addition, the final pitch angle must be equal (or near) to zero in order to continue the movement with the final value on the control variable without changes in depth.

The results are shown in Figures 2-8. Dotted lines ($\cdots$) correspond to results obtained with the *linear* model described in Section 4. Continuous lines (—) represent the evolution of the *nonlinear* model for the optimal linear controls, i.e., first iteration of the gradient method. Dashed lines (- - -) display results for the gradient method and for the set of parameters (23). We refer to this case as to *nonlinear r*. Finally, dash/dot lines (-·-·-·) show results for the gradient method and for the set of parameters as in (23) where the values for α_j are replaced by $\alpha_3 = 1$ and $\alpha_j = 0$ for $j \neq 3$, i.e., we only constraint depth $z(t)$. This last case is named *nonlinear 1.* As shown in Figures 3, 4, 6 and 7 dash/dot and dashed lines are essentially the same. However, there is a difference between them in Figures 2 and 5. Obviously, the reason for these results is that in *nonlinear r* we force the submarine to finish near to zero position on the $y-$axis. Therefore, δ_r needs to turn more than in *nonlinear 1,* where this constraint is inactive. Finally, Figure 8 shows the evolution of the cost function (with respect to the number of iterations) for the cases *nonlinear r* and *nonlinear 1.* An exponential decay is observed in both cases. We do not include pictures for the rest of state variables because they take they are not relevant in this manoeuvre.

As is typical in a gradient algorithm, results depend on the initialization. For instance, when we initiate our algorithm with zero value for $\mathbf{u}(t)$, $0 \leq t \leq T$, after convergence, we obtain different results: the costs for the case *nonlinear 1* are the same and very close to zero, but the optimal controls are slightly different; for the case *nonlinear r,* the final optimal cost is higher than in the case tested before, and the optimal controls are also different. These results seem to indicate the existence of several local minima and/or non-uniqueness of solutions.

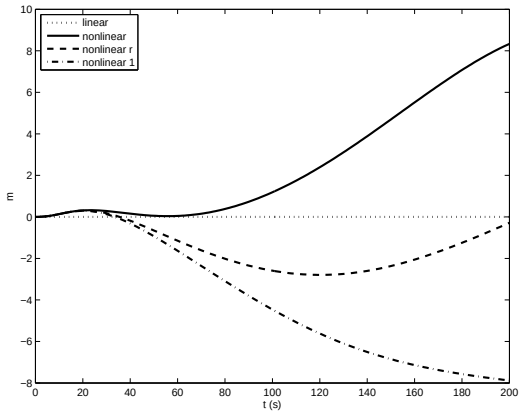

Figure 2. East movement($y(t)$)

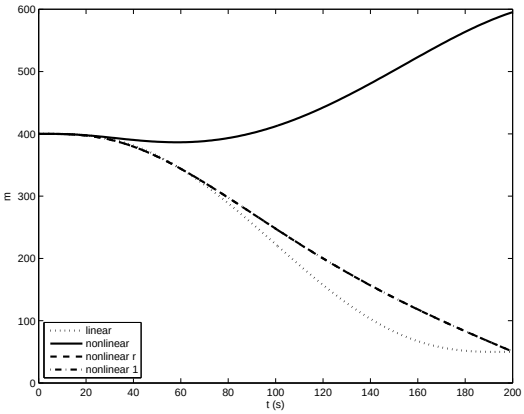

Figure 3. Depth movement($z(t)$)

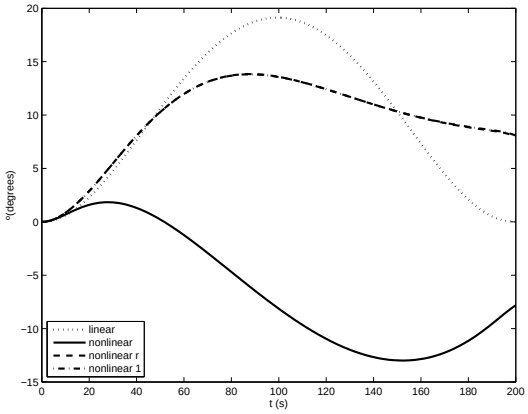

Figure 4. Pitch Angle ($\theta(t)$)

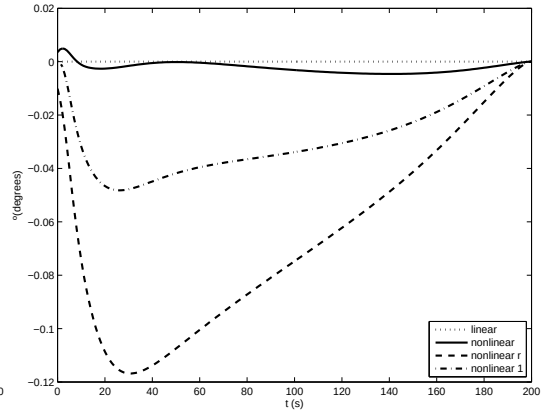

Figure 5. Deflection of rudder (δ_r(t))

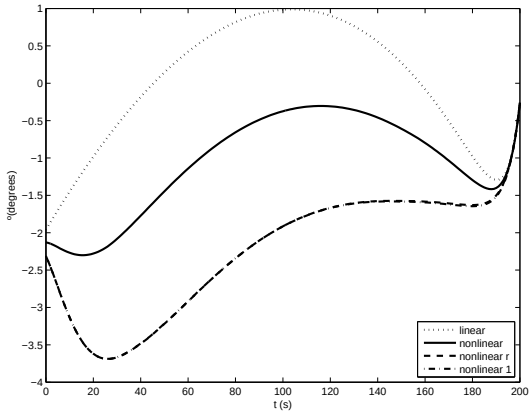

Figure 6. Deflection of stern plane ($\delta_s(t)$)

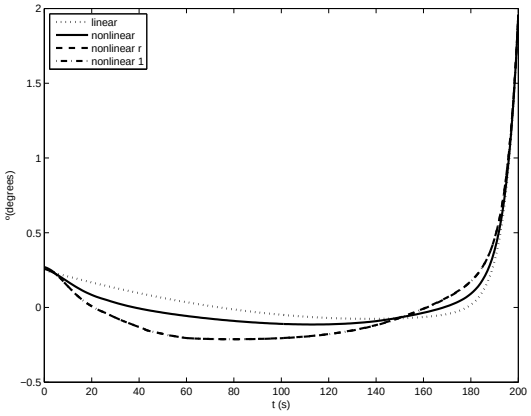

Figure 7. Deflection of bow plane ($\delta_b(t)$)

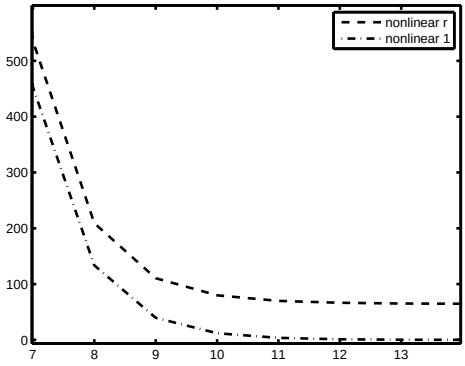

Figure 8. Cost Function

Case 2. In order to *reduce hydraulic oil consumption (and therefore noise generation)* we penalize, in addition, the L^2-norm of the control variables. Hence, now we take:

$$\begin{cases} \lambda = 0.001 \qquad \varepsilon = 10^{-6} \\ \alpha_2 = \alpha_3 = \alpha_5 = 1, \quad \alpha_j = 0, \ j \neq 2,3,5, \\ \beta_j = 1, \ j = 1,2,3 \\ \mathbf{x}\,(0) = (0,0,400,0,0,0,2.5,0,0,0,0,0) \\ \mathbf{x}^T = (0,0,50,0,0,0,0,0,0,0,0,0)\,, \quad T = 200. \end{cases} \tag{24}$$

Results are shown in Figures 9-15. We keep the same line criteria for visualization of results. The influence of the new ingredient (L^2-norm of control variable) in the cost function is mainly observed in Figures 9 and 12. In particular, deflection of rudder is more economic in this case compared to the previous situation (see Figures 5 and 12). On the contrary, we lose a little of precision in the $y\,(t)$ $-$variable (Figures 2 and 9). In what concerns the history of the cost function in terms of number of iterations, an exponential decay is also observed (Fig. 15).

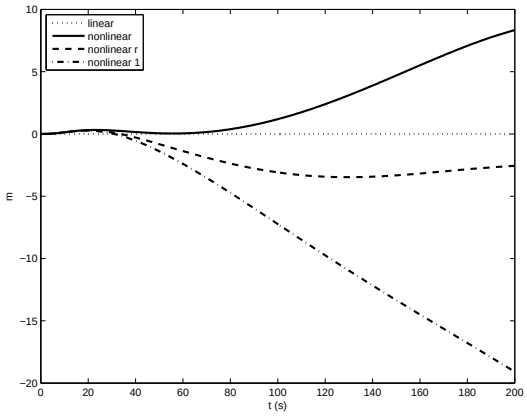

Figure 9. East movement($y(t)$)

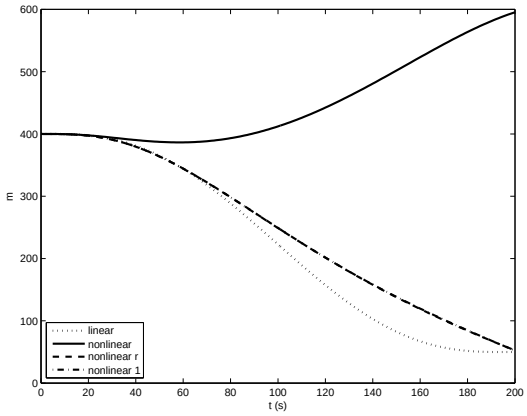

Figure 10. Depth movement($z(t)$)

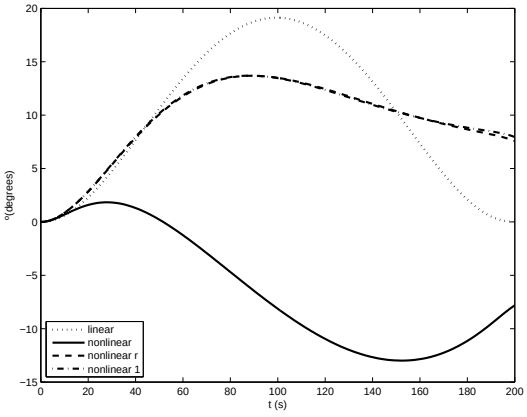

Figure 11. Pitch Angle ($\theta(t)$)

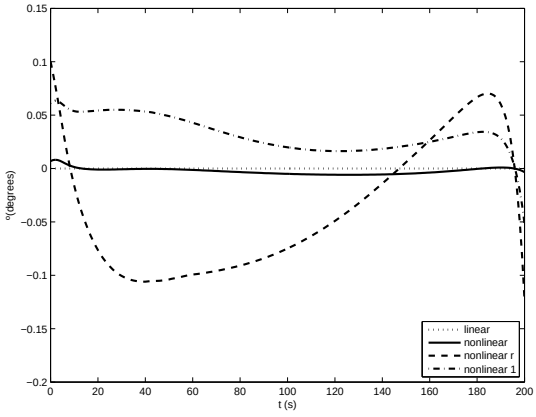

Figure 12. Deflection of rudder (δ_r(t))

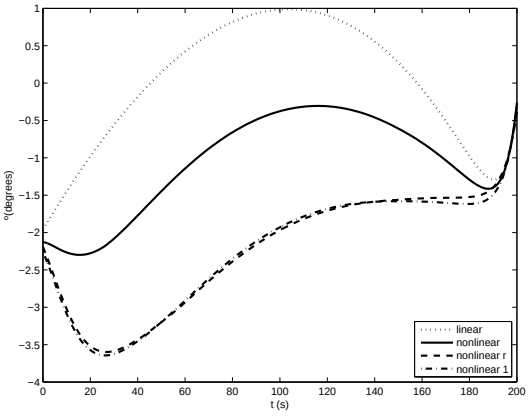

Figure 13. Deflection of stern plane ($\delta_s(t)$)

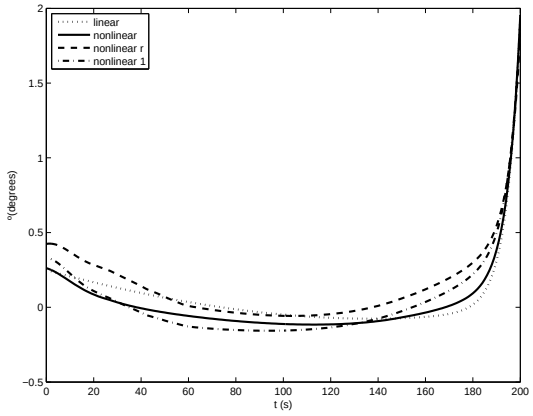

Figure 14. Deflection of bow plane ($\delta_b(t)$)

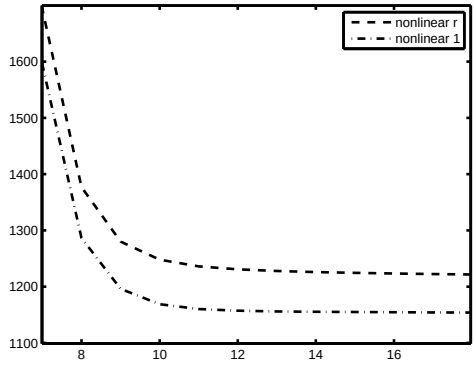

Figure 15. Cost Function

Finally, we simulate a turning manoeuvre for a constant deflection of rudder of -20^o and an average surge velocity of 7.5 m/s. This is a typical test of a *manoeuvre in a complex scenario*. The aim we pursue is precision in turning manoeuvre and, at the same time, a minimum change in vertical displacement.

In order to achieve that goal, we modified slightly the parameters Φ and F in the cost function, as follows

$$\Phi\left(\mathbf{x}\left(T\right),\mathbf{x}^{T}\right)=0 \tag{25}$$

and

$$F\left(\mathbf{x}\left(t\right),\mathbf{u}\left(t\right)\right)=\sum_{j=1}^{3}\beta_{j}\left(\mathbf{u}_{j}\left(t\right)\right)^{2}+\sum_{j=1}^{12}\delta_{i}\left(\mathbf{x}_{i}\left(t\right)\right)^{2} \tag{26}$$

with $\delta_i > 0$ another weight parameters. Now, the cost function is a commitment between a minimal expense of control on having done the corresponding manoeuvre and a minimal change on the state variables. For the turning test particulary we desire the vertical displacement to be the minimum possible. Since this type of manoeuvre is not very frequent, we do not worry about optimization with respect to controls energy. Therefore, we take:

$$\begin{cases} \lambda=0.01 \qquad \varepsilon=10^{-6} \\ \delta_3=1, \quad \delta_i=0, \quad i\neq 3, \\ \beta_j=0, \quad j=1,2,3 \\ \mathbf{x}\left(0\right)=(0,0,0,0,0,90,7.5,0,0,0,0,-1.5) \\ \mathbf{x}^{T}=(0,0,0,0,0,0,0,0,0,0,0,0)\,, \quad T=700s. \end{cases}$$

Results are displayed in figures 16 - 21. As shown by these pictures, the turning manoeuvre is very accurate, while the vertical displacement is very small. Figure 16 displays the three-dimensional turning movement. It reaches a minimum of $-2.2m$ and a peak of $0.6m$, which compared to the initial movement with $\delta_s = -1.4^o$ and $\delta_b = 0^o$ during the entire simulation time, where the minimum is $-17m$ and the maximum is $0m$, presents a reduction about the 85% on the vertical displacement.

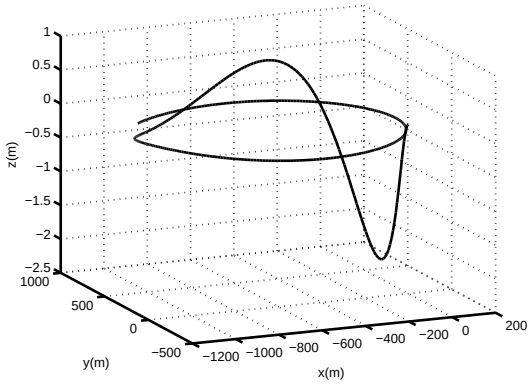

Figure 16. Three-dimensional movement

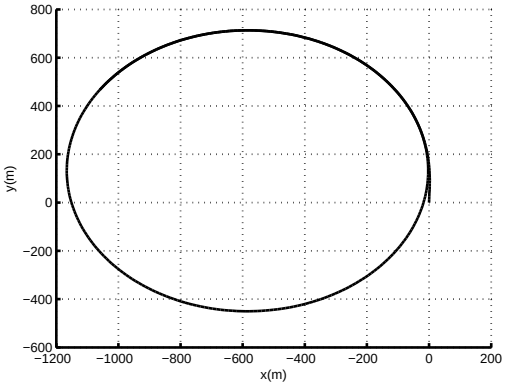

Figure 17. Movement x-y plane

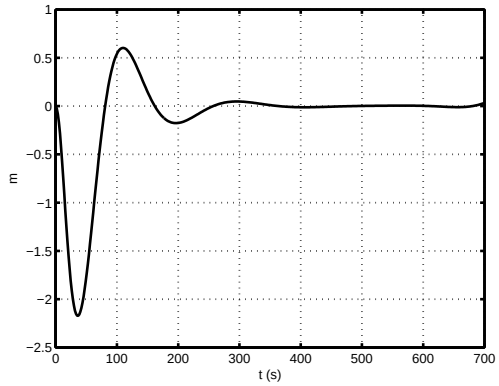

Figure 18. Depth movement ($z(t)$)

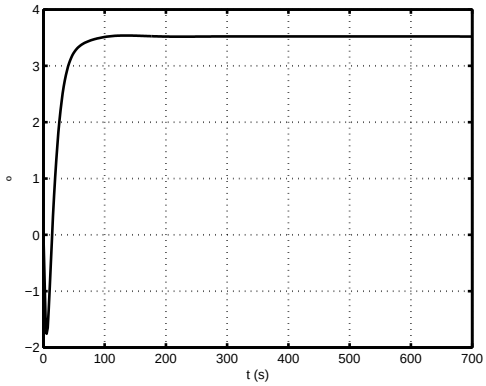

Figure 19. Roll angle (ϕ(t))

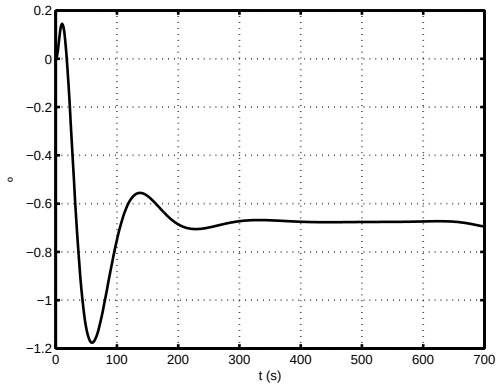

Figure 20. Pitch angle ($\theta(t)$)

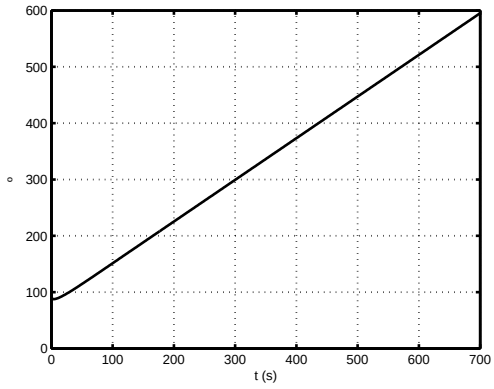

Figure 21. Yaw angle ($\psi(t)$)

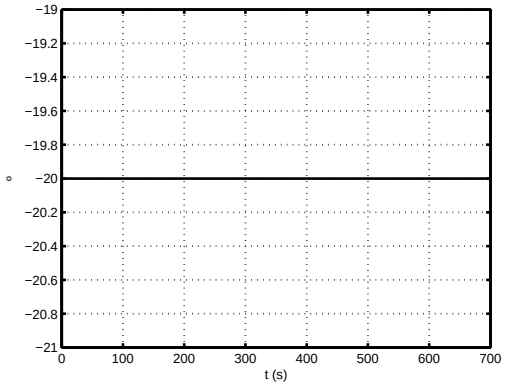

Figure 22. Deflection of rudder ($\delta_r(t)$)

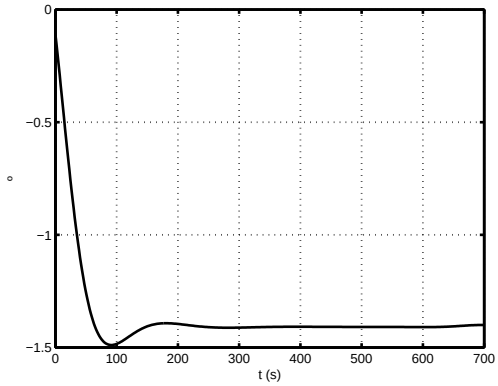

Figure 23. Deflection of stern plane ($\delta_s(t)$)

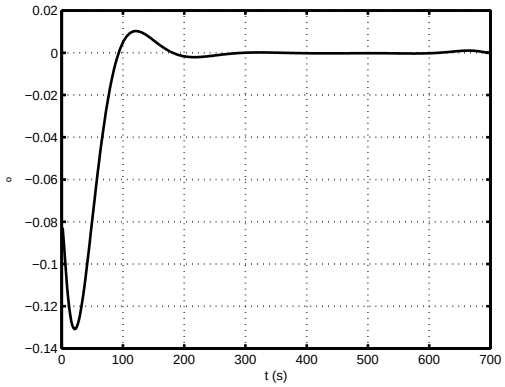

Figure 24. Deflection of bow plane ($\delta_b(t)$)

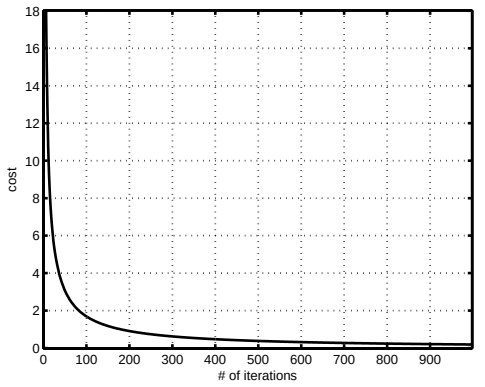

Figure 25. Cost function

6 Conclusions

The problem of manoeuvrability control for a submarine is addressed. The vehicle dynamics is modelled as a simplified version of the classical DTNSRDC equations of motion that adapts to the specific type of submarine under consideration. The manoeuvrability control problem is then formulated as a nonlinear unconstrained optimal control problem which is numerically solved by using a gradient descent method.

Numerical tests are rooted by the following three typical naval industry requirements: (1) optimality of sizing rudders, (2) minimum hydraulic consumption (and therefore minimum noise generation), and (3) reduction of vulnerability in complex scenarios. Numerical results show that, although the nonlinear model proposed in this work follows, in some sense, the same tendency as the more usual linear model, however, important changes in some state and control variables are present. As a conclusion, the nonlinearities which appear in the kinematic and dynamic equations of motion cannot be removed in order to have more accurate simulation results.

In what concerns the optimization method proposed, it allows us to obtain satisfactory simulation results in a model which presents serious mathematical difficulties.

As for the computational cost of the algorithm, for a depth change manoeuvre it takes about 60 seconds in a PC for the test cases 1 and 2. However, for the turning manoeuvre the algorithm would require some improvement (for instance, an optimal size-step method) in order to reduce time computation.

Finally, we emphasize that at the practical level it is interesting to include the propeller as a control variable and to impose some (a priori) constraints on the control variables. We plan to address these three issues as well as the more theoretical questions concerning existence and uniqueness of solutions in a future work.

7 Appendix

$m = 2352$	$l = 67$	$X_G = 0$
$Y_G = 0$	$Z_G = -0.356$	$\rho = 1.026$
$X'_{\dot{u}} = -0.00046$	$Y'_{\dot{v}} = -0.06136$	$N'_{\dot{v}} = 0.00068$
$Z'_{\dot{w}} = -0.0144$	$M'_{\dot{w}} = -0.00139$	$K'_{\dot{p}} = -7e-005$
$N'_{\dot{p}} = -3e-005$	$Z'_{\dot{q}} = -7e-005$	$M'_{\dot{q}} = -0.00098$
$K'_{\dot{v}} = -0.0006$	$Y'_{\dot{p}} = -0.0003$	$I_x = 16390$
$I_y = 659770$	$I_z = 659770$	$I_{xy} = 0$
$I_{zx} = 0$		$I_{yz} = 0$
$X'_{uu} = -0.0011$	$X'_{vv} = 0.01746$	$X'_{ww} = 0.00775$
$X'_{rp} = 0.0006$	$X'_{qq} = 0.00142$	$X'_{q\|q\|} = 0$
$X'_{rr} = 0.00208$	$X'_{vr} = 0.0224$	$Y'_{*} = 0$
$Y'_{v} = -0.06137$	$Y'_{v\|v\|} = -0.02814$	$Y'_{p} = -0.00305$
$Y'_{wp} = 0.0144$	$Y'_{pq} = 7e-005$	$Y'_{r\|r\|} = 0.00465$
$Y'_{r} = 0.0007$	$Z'_{*} = -0.0003$	$Z'_{\|w\|} = -0.002$
$Z'_{vv} = 0.185$	$Z'_{w} = -0.02028$	$Z'_{ww} = 0.02$
$Z'_{vp} = -0.01837$	$Z'_{q\|q\|} = -0.00398$	$Z'_{q} = -0.00699$
$Z'_{rr} = -0.00396$	$Z'_{vr} = -0.04513$	$M'_{*} = 2e-005$
$M'_{\|w\|} = -0.00036$	$M'_{vv} = 0.03461$	$M'_{w} = 0.00478$
$M'_{ww} = 0.00045$	$M'_{rp} = 0.00112$	$M'_{q\|q\|} = -0.00303$
$M'_{q} = -0.00389$	$M'_{rr} = -0.00119$	$M'_{vr} = -0.01573$
$K'_{*} = 0$	$K'_{v} = -0.00287$	$K'_{v\|v\|} = -0.00214$
$K'_{p\|p\|} = -0.0003$	$K'_{wp} = -0.00021$	$K'_{p} = -0.00062$
$K'_{qr} = 0.0003$	$K'_{r\|r\|} = -0.00019$	$K'_{r} = 0.00026$
$N'_{*} = 0$	$N'_{v} = -0.01864$	$N'_{v\|v\|} = 0.01868$
$N'_{p} = -0.00068$	$N'_{pq} = -0.00091$	$N'_{r\|r\|} = 0.00209$
$N'_{r} = -0.00483$	$X'_{w\|w\|} = 0$	$X'_{wq} = -0.01316$
	$M'_{vw} = 0$	
$Y'_{\delta_r} = -0.00083$	$K'_{\delta_r} = -5e-005$	$N'_{\delta_r} = -0.0012$
$X'_{\delta_r\delta_r} = -0.0039$	$X'_{\delta_s\delta_s} = -0.00119$	$X'_{\delta_b\delta_b} = -0.00299$
$Y'_{\delta_r} = -0.00083$	$Y'_{\delta_r\eta} = 0.00067$	$Z'_{\delta_s} = -0.00512$
$Z'_{\delta_s\eta} = -0.00045$	$Z'_{\delta_b} = -0.00512$	$K'_{\delta_r} = -5e-005$
$M'_{\delta_s} = -0.00231$	$M'_{\delta_s\eta} = -0.00038$	$M'_{\delta_b} = 0.00094$
$N'_{\delta_r} = -0.0012$	$N'_{\delta_r\eta} = -0.00034$	$X_B = 0$
$Y_B = 0$	$Z_B = -0.621$	$B = 23073.1$
W = 23073.1		$n = 2$

$K_{T0} = 0.525403$	$K_{TJ} = -0.338313$	$K_{TJ2} = -0.197236$
$K_{TJ3} = 0$	$K_{TJ4} = 0$	$\eta = 1.09431$
$C = 0.8976$	$K_{Q0} = 0.070405$	$K_{QJ} = -0.02846$
$K_{QJ2} = -0.033684$	$K_{QJ3} = 0$	$K_{QJ4} = 0$
$t = 0.344$	$w_f = 0.148$	$D = 3.821$
$Y'_{vwN} = -0.303$	$Y'_{v\|v\|N} = -116.2e-003$	$Z'_{w\|w\|R} = 7.7e-003$
$N'_{vwN} = -0.303$	$M'_{w\|w\|N} = -6.74e-003$	$N'_{v\|v\|N} = -18.5e-003$

References

[1] G. Allaire, Analyse numérique et optimisation, Les Éditions de l'École Polytechnique, Paris 2005.

[2] L. Byström, SSPA report n^o 2000 0101-4, for E. N. Bazan de CNM, SA, 2001.

[3] T. Chambrion and M. Sigalotti, Tracking control for an ellpsoidal submarine driven by Kirchoof's laws, IEEE Transactions on Automatic Control, 33 (1) (2008), 339-349.

[4] J. C. Culioli, Introduction à l'optimisation, Éditions Ellipses, Paris 1994.

[5] J. Felman, Revised standard submarine equations of motion. Report DTNSRDC/SPD-0393-09, David W. Taylor Naval Ship Research and Development Center, Washington D.C., 1979.

[6] E. Fernández-Cara and E. Zuazua, Control theory: History, mathematical achievements and perspectives, Bol. Soc. Esp. Mat. Apl. 26 (2003), 79-140.

[7] T. I. Fossen, Guidance and control of ocean vehicles, John Wiley and sons, 1994.

[8] J. García-Peláez, J. A. Murillo, I. A. Nieto, D. Pardo and F. Periago, Numerical simulation of a depth controller for an underwater vehicle, MARTECH'07, International Workshop on Marine Technology, Villanova i la Geltrú, 2007.

[9] M. Gertler and G. R. Hagen, Standard equations of motionfor submarine simulations, NSRDC Rep. 2510, 1967.

[10] J. N. Newman, Marine hydrodynamics, The MIT Press, Cambridge, Massachusetts, London, 1977.

[11] K. Ogata, Modern Control Engineering. Prentice-Hall, fourth edition edition, 2001.

[12] L. F. Shampine, M. W. Reichelt, The Matlab ODE Suit. SIAM Journal on Scientific Computing, vol. 18, 1997, pp 1-22.